

## Rheological phenomena of Zebra fault in South Africa goldmine by the 2011 Tohoku earthquake's surface waves

OKUBO, Makoto<sup>1\*</sup> ; OGASAWARA, Hiroshi<sup>2</sup> ; NAKAO, Shigeru<sup>3</sup> ; MURAKAMI, Osamu<sup>2</sup> ; ISHII, Hiroshi<sup>1</sup>

<sup>1</sup>TRIES, <sup>2</sup>Ritsumeikan Univ., <sup>3</sup>Kagoshima Univ.

The 2011 Tohoku earthquake was a huge earthquake. We can understand again its magnitude by large dynamic-strain observations. In general, fresh rock rupture will relieve  $10^{-4}$  strains at the source. On the other hand the 3.11 had unleashed more than  $10^{-5}$  dynamic strains to almost all of Japan. After these strain state changes, it activated seismic swarm events of Japan. On the other hand, more than  $10^{-7}$  dynamic strains had been also observed at the South Africa Republics distant from 14,000 km epicenter. Ritsumeikan university takes initiative of the projects 'Grant-in-aid : Multidisciplinary monitoring of preparation and generation of earthquakes at M2 sources in South African gold mines' and 'SATREPS: Observational Studies in South African Mines to Mitigate Seismic Risks'. In the project, we can come, we can see, we can observe at proximity micro-seismicity and/or strain field at 1-3 km depths of gold mine.

In this study, we analyzed dynamic strain records of 'Cooke4' mine, which caused by the 2011 Tohoku earthquake. Although static strain changes may be disturbed by mining activity, dynamic strain variations such as teleseismic waves and surface waves have been recorded clearly. We have estimated the strain field variations vicinity of zebra fault from two strain meter combination, and we obtained the result that dilatational strain in the fault and shear strain of both size of fault have changed by passing through the seismic waves. In presentation, we will discuss inactive fault vibration caused by teleseismic waves.

Keywords: Surface waves, Zebra fault, Dynamic strain, SATREPS

## Relationship between ESR signal intensity and grain size distribution in shear zones within the Atotsugawa fault system

FANTONG, Emilia bi<sup>1\*</sup> ; TAKEUCHI, Akira<sup>1</sup> ; KAMISHIMA, Toshio<sup>1</sup> ; DOKE, Ryosuke<sup>2</sup>

<sup>1</sup>Graduate School of Science and Engineering, University of Toyama, 3190 Gofuku, Toyama 930-8555., <sup>2</sup>Hot Spring Research Institute of Kanagawa Prefecture, 568 Iriuda, Odawara, Kanagawa 250-0031, Japan

Shear zones are zones of strong deformation within active faults and constitute significant sources of information on the seismogenic behavior of faults. The Atotsugawa fault system, which is in the Northern margin of the Hida Highland lies within a complex tectonic zone consisting of the Pacific plate, the Philippine Sea plate, the Amurian plate and the Okhotsk plate. This system consists of the Ushikubi fault, the Atotsugawa fault and the Mozumi-Sukenobe fault. The study of deformational fabrics and features within these shear zones can give more clarification on geodynamics of faults. Moreover, seismogenic behavior of a fault depends greatly on fault zone internal structure and fault rock constitutive properties. Although there are many studies on shear zone descriptions and deformational mechanisms, only few relate the description of cataclastic rocks (fault gouge) with Electron spin resonance (ESR) signals, which is based on the detection of paramagnetic defects in minerals produced by natural radiation that have accumulated for a long time and produces a characteristic signal detectable with an ESR spectrometer. By measuring the intensity of these trapped electrons, the rate of comminution and displacement of a fault can be clarified or envisaged. This study therefore focuses on the relationship between grain size distribution (sieve method) and ESR analysis, and rate of deformation with proximity to a slip plane.

Three shear zones from both the Atotsugawa and the Ushikubi fault were investigated. Sieve analysis and photomicrographs from thin sections revealed that grain size becomes coarser away from the slip plane (e.g. Fig.1a and Fig.2) indicating that the effect of displacement is more close to the slip plane. However, an irregular pattern in the grain size distribution was equally observed in some of the shear zones. This could be due to multiple phases of deformation. ESR analysis showed a decreasing trend in the intensity of signals toward the fault plane (Fig. 1b and Fig. 2) indicating that the rate of comminution was more intense towards the slip plane. However, the decreasing trend in ESR signal intensity with proximity to the slip plane was not observed in some of the shear zones probably due to multiple phase of deformation as indicated by the anatomizing faults in the shear zone II of the Ushikubi fault.

Results from ESR analysis suggest that samples closest to a slip plane will have low signal intensity than those further away while grain size distribution analyses indicates that samples closest to a slip plane become finer due to intensive crushing that is always associated with large displacement during fault activities.

Keywords: Active fault, Shear zones, ESR signal intensity, Grain size distribution, Atotsugawa fault system

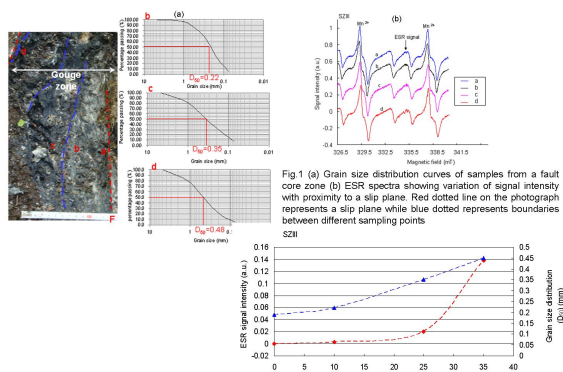


Fig.2: Relationship between ESR signal intensity and Grain size distribution. The intensity of ESR signal increases with proximity to the slip plane. By plotting the  $D_{50}$  of samples taken with proximity to the slip plane, it can be seen that grain size becomes coarser away from the slip plane.

## Physico-chemo-mechanical processes in a slip zone during the 1999 Taiwan Chi-Chi earthquake

HIRONO, Tetsuro<sup>1\*</sup> ; KAMEDA, Jun<sup>2</sup> ; KANDA, Hiroki<sup>1</sup> ; TANIKAWA, Wataru<sup>3</sup> ; ISHIKAWA, Tsuyoshi<sup>3</sup>

<sup>1</sup>Osaka Univ., <sup>2</sup>Hokkaido Univ., <sup>3</sup>JAMSTEC

To investigate the physicochemical processes of minerals during and after slip of the 1999 Taiwan Chi-Chi earthquake, we analyzed the mineral assemblages in the Chelungpu fault by using quantitative X-ray diffraction together with scanning and transmission electron microscope observations. In the primary slip zone, we found markedly low contents of quartz and clay minerals and large amounts of amorphous particles ranging in size from submicrometer to several tens of nanometers. Milling and heating experiments with host-rock samples indicated that these mineralogical changes are due to comminution and frictional heat during slip. Moreover, the changes may affect slip behavior through a mechanism such as thermal pressurization assisted by clay-mineral dehydration. In addition, preservation of a high amount of amorphous fine particles can potentially be used to identify the slip zone of the latest earthquake on not only the Chelungpu fault but also on other faults.

Keywords: mechanochemical, amorphous

## Characterization of carbonaceous materials in the Taiwan Chelungpu fault by micro FTIR-Raman spectroscopies

MAEKAWA, Yuka<sup>1</sup> ; HIRONO, Tetsuro<sup>1\*</sup> ; YABUTA, Hikaru<sup>1</sup>

<sup>1</sup>Department of Earth and Space Science, Graduate School of Science, Osaka University

Coseismic slip during an earthquake induces frictional heating in fault zone. Determination of the temperature recorded in the fault is important for estimating the dynamic shear stress and displacement during the earthquake. Here we performed micro FTIR-Raman spectroscopic analyses of carbonaceous materials from the Taiwan Chelungpu fault, which slipped at the 1999 Chi-Chi earthquake. We also conducted heating experiments and friction experiments and analyzed by FTIR-Raman spectroscopies in order to investigate the effects of fast heating rate like frictional heating during earthquake. Based on the results of analyses, we discuss the capability as new temperature proxy during the earthquake.

Keywords: Taiwan Chi-Chi earthquake, carbonaceous materials, FTIR spectroscopy, Raman spectroscopy

## Frictional properties of ground dolerite gouges at low to high slip velocities

WADA, Jun-ichi<sup>1</sup> ; KITAJIMA, Hiroko<sup>2</sup> ; TAKAHASHI, Miki<sup>2</sup> ; OOHASHI, Kiyokazu<sup>1</sup> ; INOUE, Atsuyuki<sup>1</sup> ; KANAGAWA, Kyuichi<sup>1\*</sup>

<sup>1</sup>Graduate School of Science, Chiba University, <sup>2</sup>Active Fault and Earthquake Research Center, Geological Survey of Japan

We investigated how frictional properties of ground dolerite gouges change according to grinding time. We have ground crushed and sieved grains (smaller than 500 microns) of dolerite using an automated agate mill for 10 minutes, and 6, 12, 24, 36, 48 and 60 hours. Quantitative XRD analyses indicate that amorphous phase is absent in the gouge ground for 10 minutes, but its amount increases up to 40 wt% with grinding time. Gouges ground for more than 6 hours contain abundant spherical grains composed of amorphous nano-particles. Such spherical grains are likely formed by accretion of amorphous nano-particles through their electrostatic attraction and moisture-induced binding, as accretionary lapilli. In fact, thermogravimetric analyses reveal that the amount of water adsorbed increases up to 14 wt% with grinding time in accordance with the amount of amorphous phase.

We have then conducted friction experiments on the ground dolerite gouges using a rotary shear apparatus at room temperature, a normal stress of 2 MPa, and constant slip velocities ranging from 20 micrometers/s to 1.3 m/s. At slip velocities slower than or equal to 1.3 cm/s, temperatures of gouges were lower than 70 degrees C, and steady-state friction coefficients range from 0.59 to 0.75, which tend to be higher for gouges with longer periods of grinding time at the same slip velocity. At the slip velocity of 4 cm/s, temperatures of gouges were over 100 degrees C, and steady-state friction coefficients range from 0.60 to 0.66, the difference of which among gouges with different periods of grinding time was relatively small. At slip velocities faster than or equal to 13 cm/s, however, temperatures of gouges reached higher than 180 degrees C, and steady-state friction coefficients dramatically decreased with increasing slip velocity. In addition, steady-state friction coefficients at the same slip velocity tend to be lower for gouges with longer periods of grinding time.

Such frictional properties of ground dolerite gouges depending on grinding time can be explained by the amount of water adsorbed in amorphous gouge. At slip velocities slower than or equal to 1.3 cm/s, temperatures of gouges were lower than 100 degrees C so that water adsorbed in amorphous gouge was retained. Thus, gouges ground for longer periods of time with larger amounts of adsorbed water likely became stronger in steady-state friction due to capillary bridging between amorphous gouge particles. At the slip velocity of 4 cm/s, temperatures of gouges became higher than 100 degrees C so that dehydration occurred from the amorphous gouge, which resulted in a small difference in steady-state friction among gouges with different periods of grinding time. At slip velocities faster than or equal to 13 cm/s, the moisture production rate from the dehydrated amorphous gouge was likely faster than its leak rate, which resulted in an increase in pore pressure in the gouge layer and hence a decrease in frictional strength. Thus, gouges ground for longer periods of time with larger amounts of adsorbed water became weaker in steady-state friction due to larger increases in pore pressure.

Keywords: dolerite, ground gouge, frictional properties, amorphous gouge, moisture adsorption

## Modelling of the postseismic deformation of the 2011 Tohoku Earthquake based on land and seafloor geodetic observations

IINUMA, Takeshi<sup>1\*</sup> ; HINO, Ryota<sup>1</sup> ; KIDO, Motoyuki<sup>1</sup> ; SUN, Tianhaozhe<sup>2</sup> ; WANG, Kelin<sup>3</sup> ; OHTA, Yusaku<sup>4</sup> ; OSADA, Yukihito<sup>1</sup> ; FUJIMOTO, Hiromi<sup>1</sup> ; INAZU, Daisuke<sup>5</sup>

<sup>1</sup>International Research Institute of Disaster Science, Tohoku University, <sup>2</sup>Victoria University, <sup>3</sup>Geological Survey of Canada, <sup>4</sup>Graduate School of Science, Tohoku University, <sup>5</sup>National Research Institute for Earth Science and Disaster Prevention

On 11 March 2011, the 2011 off the Pacific coast of Tohoku Earthquake (M 9.0, hereafter Tohoku Earthquake) occurred on the plate boundary between the subducting Pacific and overriding continental plates. Terrestrial and seafloor geodetic observations on and around the Japanese Islands has been clearly detecting postseismic deformation associated with the Tohoku Earthquake, although three years have passed since the main shock. Inuma et al. (2013, IAG Scientific Assembly) reported that just considering elastic response to the interplate coupling and postseismic slip on the plate boundary is insufficient to investigate the mechanical process of the postseismic deformation. We must take the inelastic deformation such as viscoelastic relaxation into account.

To tackle this problem, we estimated the displacement due to the viscoelastic relaxation by using a FEM model that includes subducting oceanic slab, difference of the viscosity between the continental and oceanic mantle, and high viscosity at the mantle wedge. The coseismic slip model based on the terrestrial and seafloor geodetic data (Inuma et al., 2012) is used to initialize the viscoelastic relaxation process. After subtracting displacements due to the large aftershocks and viscoelastic relaxation from the original displacement time series data that are measured not only with the terrestrial GPS but also GPS/Acoustic ranging and vertical displacements observed by using Ocean bottom pressure gauges, we estimated the spatial and temporal evolution of the postseismic slip distribution on the plate interface by applying a time-dependent inversion method devised by Yagi and Kikuchi (2003).

The result of FEM calculation shows that westward displacements at seafloor sites are accounted for by viscoelastic relaxation process. However, eastward movements larger than the observed displacements at the most terrestrial GPS stations are predicted by means of the FEM model. Therefore, postseismic slip (or recovery of the interplate coupling) needs account for onshore westward displacement.

One of two areas where normal-fault-type slip distributes is estimated by applying the time dependent inversion analysis to the displacement time series as well as the result of the inversion when we assume a spherical layered structure to calculate the displacements due to the viscoelastic relaxation. But, the locations of the normal-faulting areas are different. When we use the layered structure, the area is mapped inside the main rupture area of the M9 main shock. On the other hand, normal-fault-type slip at a portion of the plate boundary deeper than the coseismic main rupture area is estimated when we calculate displacements due to the viscoelastic relaxation by means of our FEM model. Since such normal faulting areas can be regarded as the patches on the plate boundary where interplate coupling occur, it is essential to estimate the locations and rates of the slip accurately to consider the frictional character on the plate interface. Therefore we need reduce and exclude the dependency of the postseismic slip distribution with respect to the estimation of crustal deformation due to the viscoelastic relaxation. We will examine and improve rheological structure that is included in the FEM model, and will present results of further investigation at the meeting.

**Keywords:** The 2011 off the Pacific coast of Tohoku Earthquake, Postseismic deformation, Viscoelastic relaxation, Postseismic slip, GPS, Seafloor crustal deformation

## Scale dependency of rock friction strength revealed by large scale biaxial friction experiment

YAMASHITA, Futoshi<sup>1\*</sup>; FUKUYAMA, Eiichi<sup>1</sup>; MIZOGUCHI, Kazuo<sup>2</sup>; TAKIZAWA, Shigeru<sup>3</sup>; KAWAKATA, Hironori<sup>4</sup>

<sup>1</sup>NIED, <sup>2</sup>CRIEPI, <sup>3</sup>Tsukuba Univ., <sup>4</sup>Ritsumeikan Univ.

In order to bridge a scale-gap between natural earthquakes ( $\sim 10^3$  m) and laboratory experiments ( $\sim 10^{-2}$  m), we carried out biaxial friction experiments using meter-sized rock specimens. We used a pair of Indian gabbro, whose nominal contact area was  $1.5 \times 0.1$  m<sup>2</sup>. The experiments were conducted under conditions with loading velocities from  $10^{-4}$  to  $3 \times 10^{-2}$  m/s and with normal stress of 1.3, 2.7 and 6.7 MPa. The normal and shear loads were measured with load cells. Hereafter, we refer the shear load divided by the normal load as the friction coefficient. It is well known that the rock friction has dependency on slip velocity at high slip velocity. We observed a similar tendency in the present experiments; the friction coefficient is almost constant ( $\sim 0.75$ ) at low loading velocities ( $10^{-4}$  to  $10^{-3}$  m/s), whereas it falls suddenly at the loading velocity of  $10^{-2}$  m/s approximately. This feature is consistent with the results using small rock specimens whose dimension is on the order of  $10^{-2}$  m (e.g. Di Toro *et al.*, 2011, Nature). It should be noted that the velocity weakening characteristics of rock friction is first confirmed on meter-sized rock. However, we found that the measured friction coefficients show weak dependency on normal stress, which suggests that the slip velocity is not a unique factor controlling the rock friction strength. On small sized rock specimens, dependency of the friction coefficient on work rate was reported; the friction coefficient is almost constant at low work rates, whereas it becomes smaller with approaching to natural conditions (e.g. Di Toro *et al.*, 2011; Mizoguchi and Fukuyama, 2010, Int. J. Rock Mech. and Min. Sci.). We investigated this relationship using the present data, and found a sudden and clear reduction of the friction coefficient at the work rate higher than  $10^{-2}$  MJ/m<sup>2</sup>s. The clear dependency of the friction on the work rate indicates that the weakening property of rock friction is governed by the work rate rather than the slip velocity. Di Toro *et al.* (2011) suggested that the work rate is proportional to a rate of temperature increase on a fault and the heating causes various transitions of rock mineral properties, which leads to the frictional weakening. In the present experiments, similar mechanisms should work and weaken the fault strength. However, we found that the meter-sized rock friction starts to decrease at the work rate one order of magnitude lower than that of the small gabbro specimens. This difference may come from the heterogeneity of the shear stress on the fault. From the point of view, we calculated heterogeneous stress distribution on the simulated fault produced by the present apparatus, and then, we estimated the weakening property of macroscopic friction depending the work rate under the estimated stress condition. We further estimated the weakening property in the case that additional stress heterogeneity was given on the fault surface. The results reveal that stronger stress heterogeneity can make more decrease in the macroscopic friction, which suggests that the rock friction has scale dependency, because such spatial heterogeneity will become strong in larger scale.

Keywords: Rock friction, Biaxial friction experiment, Scale dependency, Work rate

## Graphite-bearing pseudotachylytes in metasediment: Implication for CO<sub>2</sub> degassing by oxidation of graphite

NAKAMURA, Yoshihiro<sup>1\*</sup> ; MADHUSOODHAN, Satish-kumar<sup>2</sup> ; TOYOSHIMA, Tsuyoshi<sup>2</sup>

<sup>1</sup>Graduate School of Science & Technology, Niigata University, <sup>2</sup>Department of Geology, Faculty of Science, Niigata University

Graphite in fault rocks has important role in controlling the redox states in COH fluid, and many researchers have pointed out that the behavior of fluid in pore water or hydrous minerals dramatically change the physical and chemical property of fault rocks. Recently, the CO<sub>2</sub> degassing, from possible biogenic sources, along the faults is monitored in various active faults (e.g. Lewicki and Brantley, 2000). It is expected that the behavior of graphite in fault rocks play a key role about the fluid composition and the physicochemical properties. Here we present a detailed analysis of graphite found in pseudotachylyte and discuss the relationship between graphite and fluid during earthquake activity.

Graphite-bearing pseudotachylyte in Hidaka metamorphic belt, Hokkaido, Japan was examined using SEM, EMPA, and XRD. In pseudotachylyte-bearing cataclasite, melt-induced textures such as biotite microlites, shell textures of Fe-oxide, flow textures, spherulites and vesicles in Fe-oxide are observed. On the basis of microtextures, mineral assemblages of melted and survived minerals, pseudotachylytes are divided into two types; Pst I and Pst II. The matrix of Pst I is composed of sanidine, hematite and vesicles in Fe-oxide, and plagioclase and quartz are remained. These observations suggest that they are solidified from silicate melts by dehydration of biotite at around 700 - 1150 degree Celsius based on the experimental data. In addition, we can also deduce the stability of biotite and graphite in silicate melts of Pst I from the reaction of biotite equilibria on the T-fO<sub>2</sub> plane at 200MPa based on the experimental data of graphite and biotite. Mineral assemblages of sanidine, hematite and volatile in vesicles are stable only in high fO<sub>2</sub> fields, suggesting fO<sub>2</sub> in the range of over 10<sup>-11</sup> at around 700 degree Celsius by frictional melting of Pst I phase. In this phase, graphite in Pst I is unstable and will be converted to COH fluid in silicate pseudotachylyte melts. On the other hand, in Pst II matrix, these phyllosilicates but also quartz, plagioclase and apatite are found to be melted or have formed embayment textures, whereas only zircon has survived. These data indicate that the Pst II has formed at a peak temperature of around 1200 - 1400 degree Celsius by the breakdown of plagioclase, sulfide and apatite. The graphite content in Pst II decrease from 1.5 wt.% to 0.9 wt.% with increasing degree of frictional melting and alter the δ<sup>13</sup>C values, which shows wide range of δ<sup>13</sup>C values between -20.9 and -33.1 permil, when compared with the δ<sup>13</sup>C values of graphite from associated fault rocks and host metamorphic rocks (-24.8 +/- 0.67 permil). These data suggest that the host graphite has been converted to the COH fluids and then a part of fluid deposited graphite are re-precipitated from COH fluid during isobaric cooling and other carbon expelled as COH fluid due to the oversaturated melt.

Thus it is evident that frictional melting and dehydration of sheet silicates during coseismic slip generates CO<sub>2</sub> gas by the oxidation of carbonaceous materials. During the transformation of cataclasite to pseudotachylyte the total carbon content has decreased by about 0.5 wt.%. Assuming a rock density of 2.7g / cm<sup>3</sup>, the fusion of 10<sup>-3</sup> m<sup>3</sup> (i.e. 1mm thickness × 1m<sup>2</sup> fault plane) of cataclasite into Pst II releases 50g of excess CO<sub>2</sub>. The estimation of CO<sub>2</sub> degassing in this study is comparable to those reported by Famin et al. (2008). Thus, not only carbonates but also organic matters, including graphite and carbonaceous materials in crustal rocks, are potential to be a source of CO<sub>2</sub> by frictional melting, and the release of CO<sub>2</sub> into fault planes may drastically change the dynamic properties of flash fluid pressure and frictional properties of fault planes during seismic activity.

Reference: Famin. et al., 2008. EPSL, 265, 487-497. Lewicki. & Brantley., 2000. GRL, 27(1), 578.

Keywords: Graphite, Pseudotachylyte, Carbon isotopes, Frictional melting, CO<sub>2</sub> degassing

## Nanograins and carbonaceous film on a fault surface: an example from a fossil megasplay fault in the subduction zone

KITAMURA, Yujin<sup>1\*</sup> ; KIMURA, Gaku<sup>2</sup> ; KAMEDA, Jun<sup>4</sup> ; KOUKETSU, Yui<sup>5</sup> ; YAMAGUCHI, Asuka<sup>6</sup> ; KAGI, Hiroyuki<sup>5</sup> ; HAMAHASHI, Mari<sup>2</sup> ; FUKUCHI, Rina<sup>2</sup> ; HAMADA, Yohei<sup>3</sup> ; FUJIMOTO, Koichiro<sup>7</sup> ; HASHIMOTO, Yoshitaka<sup>8</sup> ; SAITO, Saneatsu<sup>3</sup> ; KAWASAKI, Ryoji<sup>2</sup> ; KOGE, Hiroaki<sup>2</sup> ; SHIMIZU, Mayuko<sup>2</sup> ; FUJII, Takenao<sup>9</sup>

<sup>1</sup>Dept. Earth and Environmental Sci., Kagoshima University, <sup>2</sup>Dept. Earth and Planet. Sci., University of Tokyo, <sup>3</sup>IFREE, JAMSTEC, <sup>4</sup>Dept. Nat. Hist. Sci., Grad. Sch. Sci., Hokkaido University, <sup>5</sup>Geochem. Research Center, University of Tokyo, <sup>6</sup>Atmosph. Ocean Research Institute, University of Tokyo, <sup>7</sup>Tokyo Gakugei University, <sup>8</sup>Kochi University, <sup>9</sup>SHIMADZU Corp.

Friction on the fault plane controls the behavior of faulting during seismic slip. Recent studies suggest that the frictional process on faults shows scale dependency. It is critically important to observe structures on the fault planes in various scales, especially in smaller scale in the sub-micron range. The roughness on fault planes has long been thought to hold fractal property, however, a recent work observed that a mirror fault plane, when examined up to nanometer-scale, does not obey self-affine roughness. Their observation revealed that the fault surface is coated by grains of several ten nanometers in diameter. In this abstract, we show a detailed observation of a glossy fault plane with striations sampled from drilled core of the Nobeoka Thrust taken by a scientific drilling project, the Nobeoka Thrust Drilling Project (NOBELL).

The NOBELL recovered cores with a total depth of 255 m penetrating the Nobeoka Thrust at 41 m below ground surface. The visual observation of the cores and the wireline log of the borehole clearly differentiate the hanging wall and the footwall. In this study, we analyzed a fault plane just below the Nobeoka Thrust main fault core on which gloss and striation develop using an integrated apparatus of Confocal Laser Scanning Microscope (CLSM) and Atomic Force Microscope (AFM). We also analyzed the sample surface applying Raman spectroscopy, Auger electron spectroscopy (AES) and organic component analysis using CHN coder (Yanaco MT-6).

The sample surface was imaged by the CLSM and AFM in various scale and its topography was obtained. The grains of several tens of nanometers in diameter were observed under the AFM image. This surface shows very flat surface with a height difference of ~80 nm in the imaged square ten micrometers on a side. The X-Z measurement by CLSM revealed an interface of around 1 micrometer below the surface. The interference fringe was observed at the rim of dark area. These facts suggest that the fault surface is covered by a thin film approximately 1 micrometer thick. The result of the Raman spectrometry indicates that the glossy fault plane material is rich in carbon. The organic component analysis of handpicked samples reported carbon fraction. Applying the AES, we recognized carbonaceous material on the true surface.

In conclusion, the questioned sample here appears to have been polished with fault frictional process so intensely that the surface grains comminuted to sub-micrometers and then a thin carbonaceous film developed. Such nanoscale structure observations in combination with the geometrical fractal property and chemical and surface analysis could provide further details of dynamic weakening during seismic slip.

Keywords: Nobeoka Thrust Drilling Project, subduction zone, accretionary prism, Shimanto belt, fault weakening, fault mirror

## Dynamic backthrust branching: role of barriers, and implications

XU, Shiqing<sup>1\*</sup> ; FUKUYAMA, Eiichi<sup>1</sup> ; BEN-ZION, Yehuda<sup>2</sup> ; AMPUERO, Jean-paul<sup>3</sup>

<sup>1</sup>NIED, <sup>2</sup>University of Southern California, <sup>3</sup>California Institute of Technology

Increasing evidence indicates that backthrusts may become active during or after megathrust ruptures in subduction zones, such as in Chile and Sumatra (Melnick et al., 2012; Singh et al., 2011). Previous studies of relevant mechanisms mainly focused on the interaction between forethrusts and the megathrust. Here we investigate through dynamic rupture simulations how backthrusts may be activated by megathrust ruptures in subduction zone environments. Assuming a single backthrust branch that is backward inclined to the compressional side of a continuous main fault, our results show that (1) fast speed and long propagation distance of the main rupture favor the activation of backthrust; (2) the outward propagation of the activated branch rupture interacts with the main fault mainly in the backward direction, while the tapered slip towards the branch end at the junction affects the main rupture behavior around the junction. We further assume an effective barrier for the main fault at the junction, motivated by the previous studies that barriers of various types (e.g. sharp fault bend, fault end, and transition region with increased basal friction) can also generate backthrusts during the long-term quasi-static process. Compared to the case without barrier, one prominent effect of the barrier is to arrest or delay the forward propagation of the main rupture, such that a resultant backward stress lobe as discussed in Xu and Ben-Zion (2013) can load the backthrust branch over a considerable time. This is particularly important for rupture activation along relatively immature backthrusts within sediments, where the nucleation time leading to the spontaneous propagation phase could be long, due to the large effective  $D_c$ , low frictional strength drop, or surface roughness. Indeed, our additional results confirm that the barrier model, although not always necessary, is more favorable for the activation of backthrusts with increased dynamic friction.

Our study has several implications: (i) it agrees with the quasi-static model based on the critical taper theory and limit analysis (Cubas et al., 2013) that an increase of basal friction towards the toe may statistically favor the activation of backthrusts near the up-dip limit of megathrust ruptures; (ii) there are also possibilities that backthrusts can still be activated by a propagating rupture, therefore the dynamic critical taper theory developed by Wang and Hu (2006) needs to be improved. In fact, not only the region near the up-dip limit of the seismogenic zone can be pushed into a critical state, successive region around the propagating rupture front within the seismogenic zone can also be temporarily stressed to failure and may even sustain a failure propagation along preexisting branches; (iii) it provides a specific example of compressional-side antithetic branching that can support the early speculation of fault behavior at junctions (King, 1986; Andrews, 1989).

Keywords: earthquake branching, friction of fault zones, fault barrier

## A possibility of a CM fault thermometer Part 1: Reflectances

OKAMOTO, Shiori<sup>1</sup> ; HOSHINO, Kenichi<sup>2\*</sup>

<sup>1</sup>Fac. Sci., Hiroshima Univ., <sup>2</sup>Grad. Sch. Sci., Hiroshima Univ.

The chemical kinetics of thermal maturation (coalification) of carbonaceous matters (CMs) in the oil and gas windows was well investigated by Burnham and his coworkers (e.g., Braun and Burnham, 1987). Burnham and Sweeney (1989) and Sweeney and Burnham (1990) introduced an activation energy distribution model for their rate law of dehydration and degassing of CMs and presented the correlation between the reflectance of CM in oil (%Ro, in percent) and the extent of the reaction (F) calculated from the rate law. They also noted that the rate law can be applied for heating rates ranging from laboratory conditions (1C/week), igneous intrusions (1C/day), and geothermal systems (10C/100 yr) to burial diagenesis (1C/10 m.y.).

On the other hand, Huang (1996) demonstrated that %Ro increased after a few days heating experiments and estimated a power rate law with  $t$  (second) to the power of 0.078. Muirhead et al. (2012) also examined that R1 ratios of Raman spectra of CMs increased after a few tens-seconds pyrolysis and proposed a power rate law with the power depending on  $T$  (K). However, those power rate laws were obtained from the experiments with bare CM fragments extracted from rocks. The power rate laws may not be applied to CMs in rocks, since we confirmed that the R1 ratios of CMs on surfaces of heated rock samples are larger than those inside the samples (details will be shown in the following presentation, Part 2).

Chips of pelitic rocks collected from the Shimanto accretionary complex were heated in an Ar-purged capsule in an oven. Since the oven takes 18-21 minutes to achieve pre-set steady temperatures and a few minutes for cooling down after heating, the following heating durations are regarded as those of constant temperatures during heating runs. The chips were heated at temperatures, 300, 350, 450, 550, 600 and 750C for 2, 5, 13 and 34 minutes.

Reflectance measurements and Raman spectroscopic analyses were taken for CMs in the chips of which surfaces were scraped off before polishing. The reflectances in air ( $R_a$ , not in percent) of CMs of unheated and heated chips and standards (SiC, GGG, YAG, sapphire and spinel) were obtained by analyzing gradations of G color of 24 bit color microphotographs taken by a reflecting microscope.

Averages of  $R_a$  of CMs in two unheated chips are 0.093 and 0.106, while an average of measured %Ro of the former is 1.99 of which  $F$  (extent of reaction) calculated from the correlation of Sweeney and Burnham (1990) is 0.618.  $R_a$  values of CMs in chips heated below 450C show no significant difference with those in unheated ones. This is consistent with that  $F$  simulated along the  $T$ - $t$  paths of the 300C, 350C and 450C for 34 minutes runs are 0.618, 0.618 and 0.622, respectively.

On the other hand, averages of  $R_a$  of CMs heated at 550C, 600C and 750C for 34 minutes are 0.121, 0.127 and 0.151, respectively, and their respective  $F$  values simulated are 0.742, 0.811 and 0.850. It is interesting that the averages of  $R_a$  for the runs at 750C for 2, 5 and 13 minutes are 1.47, 1.50 and 1.50, respectively. The all simulated  $F$  values for the last three runs are 0.850, the maximum extent of reaction of the rate law.

Although additional heating experiments of rocks with CMs of various initial maturities are needed, we may say from the above results that the CM fault thermometer is quite possible for high temperature faulting.

CM maturations due to heating indicated by Raman spectra will be shown in the following presentation (Part 2).

Keywords: carbonaceous matter, thermometer, fault, reflectance

## A possibility of a CM fault thermometer Part2: Raman spectra

OKAMOTO, Shiori<sup>1\*</sup> ; KOUKETSU, Yui<sup>2</sup> ; SHIMIZU, Ichiko<sup>3</sup> ; HOSHINO, Kenichi<sup>4</sup>

<sup>1</sup>Fac. Sci., Hiroshima Univ., <sup>2</sup>Univ. Tokyo, Grad. Sch. Sci., <sup>3</sup>Univ. Tokyo, Grad. Sch. Sci., <sup>4</sup>Grad. Sch. Sci., Hiroshima Univ.

A possibility of a CM fault thermometer Part2: Raman spectra

OKAMOTO, Shiori, KOUKETSU, Yui, SHIMIZU, Ichiko, HOSHINO, Kenichi

Key words: carbonaceous matter, thermometer, fault, Raman spectra

Parameters of Raman spectra of carbonaceous matters (CMs) have been widely used to estimate geological temperatures (e.g., Beyssac et al., 2002). Huang (1996) and Muirhead et al. (2012) proposed empirical power rate laws for CM maturation represented by reflectances in oil (%Ro) and R1 ratios of Raman spectra, respectively, from pyrolytic experiments of bare CM fragments extracted from rocks and meteorites, respectively.

To investigate a possibility of a fault thermometer by thermal maturations of CMs indicated by their Raman spectra, we conducted heating experiments of pelitic rock samples taken from Aki Group of the Shimanto accretionary belt in Kochi Prefecture, whose diagenetic temperature is estimated as ~180°C by vitrinite reflectances (Kitamura et al., 2014). The samples were heated at temperatures, 300, 350, 450, 550, 600 and 750°C for 2, 5, 13 and 34 minutes (see details in the previous presentation, Part 1).

It was indicated by comparing the spectra of CMs on surfaces of heated samples and those inside the sample that maturations of the former proceeded faster than the latter during heating. Therefore, in order to apply the thermal maturation of CM to a fault thermometer, it is needed to analyze CMs inside the samples.

It should be mentioned that micro-XRD analyses of CMs after the highest and longest heating run show no graphite peak. Hence, the maturation process during the present experiments is not graphitization but coalification.

Raman spectra of CMs show two major peaks, so-called G-band and D1-band peaks. Analytical results of the peaks indicate that certain parameters of Raman spectra of CMs remarkably vary even after low temperature (300 - 450°C) heating runs, whereas reflectances of CMs do not increase (see Part 1). The positions of G-band peak (Gp) and D1-band peak (Dp) tend to shift toward higher wave numbers with increasing heating durations in the all temperature runs. However, they do not shift monotonically with heating temperatures. Their wave numbers increase with the heating temperatures up to 450°C, then decrease at 550°C, and again increase up to 750°C.

Differences between Gp and Dp (Gp-Dp) also vary with heating temperatures and durations. Although they become smaller as the temperature is higher for the longest runs (34 minutes), this temperature dependency could not be seen for the other heating durations.

The ratio of intensity to full width at half maximum of the G-band peak (Gif) and that of the D1-band peak (Dif) decrease with increasing temperatures from 300°C to 450°C and from 550°C to 750°C, but increase from 450°C to 550°C. The both Gif and Dif do not show monotonic change with the heating durations.

As stated in the above, a simple indicator varying monotonically with heating temperatures and durations has not been found yet. However, we conceive that the sensitivities of the above indices of the Raman spectra to the thermal maturation of CM may show their potentials as a fault thermometer. Size dependencies of variations in some of the above indices with heating temperatures and durations and similarities of those of small-grained CMs and rims of large-grained ones also show a possibility to estimate both heating temperature and duration simultaneously by a size dependent thermometer, that is, a thermo-chronometer.

Keywords: carbonaceous matter, thermometer, fault, Raman spectra

## Mineral characteristics of the plate-boundary fault at the Japan Trench

KAMEDA, Jun<sup>1\*</sup> ; SHIMIZU, Mayuko<sup>2</sup> ; UJIIE, Kohtaro<sup>3</sup> ; HIROSE, Takehiro<sup>4</sup> ; IKARI, Matt<sup>5</sup> ; REMITTI, Francesca<sup>6</sup> ; MORI, James<sup>7</sup> ; CHESTER, Frederick<sup>8</sup> ; KIMURA, Gaku<sup>2</sup>

<sup>1</sup>Hokkaido University, <sup>2</sup>University of Tokyo, <sup>3</sup>Tsukuba University, <sup>4</sup>JAMSTEC, <sup>5</sup>University of Bremen, <sup>6</sup>Universita di Modena, <sup>7</sup>kyoto University, <sup>8</sup>Texas A&M University

The rupture and slip of the 2011 Tohoku-oki earthquake (Mw9.0) propagated along the plate-boundary megathrust and caused a huge tsunami. In order to elucidate the physical mechanisms responsible for such unexpectedly large slip of the fault, the IODP Exp. 343, the Japan Trench Fast Drilling Project (JFAST) was carried out one year after the earthquake. It succeeded in recovery of material from the plate boundary shear zone. We have examined how mineralogical properties vary through a depth-section including the plate boundary fault rock.

At the drill site (C0019E) where the large fault slip (>50m) occurred, a plate boundary shear zone was identified around 820 mbsf. X-ray diffraction (XRD) analysis revealed that abundance of smectite is markedly higher within the fault (60-80 wt.%) than in the surrounding host rocks, suggesting the shear zone material had a low intrinsic friction coefficient. Laboratory experiments on these materials demonstrated very low frictional state under various sliding conditions (Ujiie et al., 2013; Ikari et al., submitted)

In comparison, we also examined the mineralogy of reference material recovered on the outer rise of the Japan Trench (Site 436) during DSDP Leg 56. XRD analyses on the continuous series of cores found a marked anomaly in smectite abundance in the topmost ~5m section in the pelagic clay layer. Such a mineralogical feature compares well to that observed in the JFAST cores, and the smectite-rich horizon in the incoming sediments is inferred to be the localized deformation zone (decollement) when it arrives at the Japan Trench.

Keywords: Japan Trench, smectite, pelagic clay, Tohoku-oki earthquake

## Shock compression experiment of olivine- Part 3: pulverization occurred before frictional melting

OBATA, Masaaki<sup>1\*</sup>; MASHIMO, Tsutomu<sup>2</sup>; CHEN, Liliang<sup>2</sup>; ANDO, Jun-ichi<sup>3</sup>; YAMAMOTO, Takashi<sup>3</sup>; UEDA, Tadamasu<sup>1</sup>

<sup>1</sup>Graduate School of Science, Kyoto University, <sup>2</sup>Institute of Pulsed Power Science, Kumamoto University, <sup>3</sup>Graduate School of Science, Hiroshima University

Seismic waves may be generated by a rapid slip accompanied by a rapid drop of shear stress at or near the rupture tip that propagates rapidly. It is an important subject of seismology to identify the material changes occurring at the fracture tip. The inferred slip weakening has been ascribed to (1) frictional melting and lubrication, (2) thermal pressurization, (3) flash heating and melting, (4) powder lubrication, and the combinations of those above. High-speed rotary shear friction apparatus has played important roles in formulating the above hypothesis in the past, but in these experiments fault planes are already prepared and the formation of new fault planes cannot be studied. Moreover normal pressure cannot exceed few tens of mega-Pascal because of the instrumental limitation.

We performed a series of shock compression experiments using a keyed powder gun at Kumamoto University in order to investigate the focal mechanics of deep earthquakes. We used a single crystal of forsterite (Fo 94; shaped in a diskette of diameter 12 mm and thickness 3 mm nearly perpendicular to the olivine *c*-axis). The olivine disk is mounted in a steel capsule. Flyer speed was 1.5 km/s; applied pressure, 31 GPa; and shock wave velocity, ca. 7 km/s; particle velocity, ca. 1 km/s. After the shock experiment the capsule is recovered from the gun and cut perpendicular to the disk plane and polished thin sections were prepared for optical, SEM and TEM observations.

Many shear planes were generated. Olivine shows wavy extinctions and locally cataclastic texture. Shear planes (i.e., fault) are typically sharp and show up to 0.5 mm displacement. The TEM observation of the fault wall where 'spongy material is attached' revealed that the wall has a zonal structure as follows. Well inside the wall are developed densely spaced and tangles [001] screw dislocations. Outer 2-5 micron zone is polycrystalline olivine of average grain size 200-300 nm. The outermost rim is an aggregate of semi-rounded small olivine particles (ca. 200 nm) mounted in a matrix of glass of olivine composition, indicating that melting of olivine occurred here. It is important to note that the same dislocation structure remained in these olivine nano-particles. It is inferred from these structure that polygonization and pulverization of olivine has occurred before melting began near the fault wall (within a few microns). Such pulverization is possible at running fracture tip, where stress and strain rate are the highest (Reches and Dewar, 2005). The whole process occurred in a short duration of the order of 0.5 microsecond. The fracturing was probably propelled by the rapid sweep of shock waves running through the sample in our experiment. Apart from the role of the shock waves, the situation is considered to be analogous to natural earthquakes. Present experimental result sheds light on the long-lasting controversy on the formation of pseudotachylytes.

Reference: Reches and Dewers (2005) Gouge formation by dynamic pulverization during earthquake rupture. *EPSL* 235, 361-374.

Keywords: shock compression experiment, olivine, frictional melting, pulverization, fault, earthquake

## High-velocity frictional behaviors of dolerite under controlled pore-water pressure

TOGO, Tetsuhiro<sup>1\*</sup>; SHIMAMOTO, Toshihiko<sup>1</sup>; MA, Shenli<sup>1</sup>; YAO, Lu<sup>1</sup>

<sup>1</sup>Institute of Geology, China Earthquake Administration

High-velocity friction experiments on rocks with or without gouge have been conducted mostly under dry conditions and demonstrated dramatic weakening of faults at high velocities (e.g., Di Toro et al., 2011, *Nature*). Recent experiments under wet conditions (e.g., Ujiie and Tsutsumi, 2010, *GRL*; Faulkner et al., 2011, *GRL*) revealed very different behaviors from those of dry faults, but those experiments were done under drained conditions. Experiments with controlled pore pressure  $P_p$  are definitely needed to determine mechanical properties of faults under fluid-rich environments such as those in subduction zones. Thus we have developed a pressure vessel that can be attached to our rotary-shear low to high-velocity friction apparatus (Marui Co Ltd., MIS-233-1-76). With a current specimen holder, friction experiments can be done on hollow-cylindrical specimens of 15 and 40 mm in inner and outer diameters, respectively, at controlled  $P_p$  to 35 MPa, at effective normal stresses of 3-9 MPa, and at slip rates of 60 mm/year to 2 m/s. An effective normal stress can be increased by about 10 times by replacing a 10 kN pneumatic actuator with a 100 kN hydraulic actuator. We report an outline of the experimental system and preliminary high-velocity experiments with controlled pore pressure on Shanxi dolerite.

High-velocity friction experiments were performed on hollow-cylindrical specimens of Shanxi dolerite at effective normal stresses of 0.13-1.07 MPa and at slip rates of 1, 10, 100 and 1000 mm/sec. Nitrogen gas and water were used of the pore fluid and compared the frictional behavior. In the  $N^2$  tests an axial force was kept at 1 kN and the nitrogen gas pressure was increased in steps from 0 to 5 MPa to change an effective normal stress. In the wet tests the specimens were soaked in distilled water in the vessel and  $P_p$  was applied by nitrogen gas in a similar manner as in the dry tests. Nitrogen gas acted as buffer to prevent an abrupt change in the pore-water pressure during experiments. The steady-state friction coefficient of dry dolerite increased from 0.3-0.35 at 10 mm/s to 0.55-0.8 at 100 mm/s and then decreased down to 0.2-0.6 at 1000 mm/s. The results are quite similar to those of dry granite tested under similar conditions (Reches and Lockner, 2010, *Nature*). However, the steady-state friction coefficient of dolerite under a pore-water pressure decreased monotonically from 0.4-0.8 at 1 mm/s to 0.3~0.5 at 1000 mm/s, and the strengthening from 10 to 100 mm/s disappeared with a pore-water pressure. We plan to conduct more experiments with controlled pore-water pressure and to do textural and material analysis of specimens to gain insight on the weakening mechanisms.

Keywords: High-velocity friction experiment, Pore-water pressure